Available online at www.sciencedirect.com

ScienceDirect

Journal of Nutritional Biochemistry 39 (2017) 156–168

Journal of Nutritional Biochemistry

Chronic exposure to short-chain fatty acids modulates transport and metabolism of microbiome-derived phenolics in human intestinal cells☆

Evelien Van Rymenant[a], László Abrankó[b], Sarka Tumova[b], Charlotte Grootaert[a], John Van Camp[a], Gary Williamson[b], Asimina Kerimi[b,*]

[a]Department of Food Safety and Food Quality, Faculty of Bioscience Engineering, University of Ghent, 9000 Gent, Belgium
[b]School of Food Science and Nutrition, University of Leeds, Leeds LS2 9JT, UK

Received 17 August 2016; received in revised form 23 September 2016; accepted 27 September 2016

Abstract

Dietary fiber-derived short-chain fatty acids (SCFA) and phenolics produced by the gut microbiome have multiple effects on health. We have tested the hypothesis that long-term exposure to physiological concentrations of SCFA can affect the transport and metabolism of (poly)phenols by the intestinal epithelium using the Caco-2 cell model. Metabolites and conjugates of hesperetin (HT) and ferulic acid (FA), gut-derived from dietary hesperidin and chlorogenic acid, respectively, were quantified by LC-MS with authentic standards following transport across differentiated cell monolayers. Changes in metabolite levels were correlated with effects on mRNA and protein expression of key enzymes and transporters. Propionate and butyrate increased both FA transport and rate of appearance of FA glucuronide apically and basolaterally, linked to an induction of MCT1. Propionate was the only SCFA that augmented the rate of formation of basolateral FA sulfate conjugates, possibly *via* basolateral transporter up-regulation. In addition, propionate enhanced the formation of HT glucuronide conjugates and increased HT sulfate efflux toward the basolateral compartment. Acetate treatment amplified transepithelial transport of FA in the apical to basolateral direction, associated with lower levels of MCT1 protein expression. Metabolism and transport of both HT and FA were curtailed by the organic acid lactate owing to a reduction of UGT1A1 protein levels. Our data indicate a direct interaction between microbiota-derived metabolites of (poly)phenols and SCFA through modulation of transporters and conjugating enzymes and increase our understanding of how dietary fiber, *via* the microbiome, may affect and enhance uptake of bioactive molecules.

Keywords: Gut metabolism; Short-chain fatty acids; Polyphenol; Phase II metabolism; Transporter

1. Introduction

The gut microbiome-nutrition-obesity axis has become a key focus of recent translational research and accumulating studies show that microbial metabolites are important regulators of the intestinal epithelial barrier, shaping gut immunity [1]. The gut is host to more than 100 trillion cells and 5 million unique genes coding for enzymes that ferment dietary fiber to large quantities of short-chain fatty acids (SCFA), the preferential source of energy for colonocytes [1–3]. The ratio of the main SCFAs, acetate, propionate and butyrate, is altered by consumption of prebiotics and certain drugs [3–6]. Several health benefits have been proposed for SCFA, including prevention of intestinal inflammation, reduction of colon cancer risk, stimulation of satiety and hypolipidemic effects [3,7–10]. Lactate, another microbial product resulting from the fermentation of dietary polysaccharides, is found at lower concentrations than SCFA as it is further oxidized by cross-feeding but can still reach 5 mM in the gut lumen of healthy individuals [11]. The MCT1 transporter is mainly responsible for absorption of luminal SCFA [12–15] in colonocytes and is also

Abbreviations: ABCC, ATP-binding cassette sub-family C; ABCG2, ATP-binding cassette sub-family G member 2 (BCRP); DHFA, Dihydroferulic acid; DMCA, 3,4-dimethoxycinnamic acid; FA, Ferulic acid; FA-glu, Ferulic acid-4-*O*-glucuronide; FA-sul, Ferulic acid-4-*O*-sulfate; HT, Hesperetin; HT-7-glu, Hesperetin-7-*O*-glucuronide; HT-3′-glu, Hesperetin-3′-*O*-glucuronide; HT-7-sul, Hesperetin-7-*O*-sulfate; HT-3′-sul, Hesperetin-3′-*O*-sulfate; SA, Salicylic acid; SCFA, Short-chain fatty acids; SULT, Sulfotransferase; UGT, Uridine diphosphate-glucuronosyl transferase.

☆ Chemical compounds studied in this article: Dihydroferulic acid (PubChem CID: 14340); Ferulic acid (PubChem CID: 445858); Hesperetin (PubChem CID: 72281); Ferulic acid-4-*O*-glucuronide (PubChem CID: 6443140); Ferulic acid-4-*O*-sulfate (PubChem CID: 6305574); Hesperetin-3′-*O*-glucuronide (PubChem CID: 46896123); Salicylic acid (PubChem CID: 338).

* Corresponding author at: School of Food Science and Nutrition, University of Leeds, Leeds LS2 9JT, UK. Tel: +44-113-3438380.

E-mail addresses: evelien.vanrymenant@ugent.be (E. Van Rymenant), l.abranko@leeds.ac.uk (L. Abrankó), s.tumova@leeds.ac.uk (S. Tumova), charlotte.grootaert@ugent.be (C. Grootaert), john.vancamp@ugent.be (J. Van Camp), g.williamson@leeds.ac.uk (G. Williamson), a.kerimi@leeds.ac.uk (A. Kerimi).

http://dx.doi.org/10.1016/j.jnutbio.2016.09.009

involved in lactate transport [16,17]. Apart from being substrates, SCFA can also modulate transporter expression and, for example, enhance MCT1 function as shown in several intestinal cell models [12,18,19]. In pig colon, resistant starch consumption raised SCFA concentrations in the gut, followed by an up-regulation of MCT1 [4], while MCT1 expression was increased in the rat intestine after pectin feeding, although no data were reported regarding SCFA content in the gut [20]. These studies indicate that diet can influence SCFA production in the gut and promote their uptake by regulation of transporter expression in the gut epithelium.

Polyphenols are a broad class of compounds, including monophenolic hydroxycinnamic acids and multiphenolic flavonoids, and will be referred to here as (poly)phenols. They have biological effects on health biomarkers in humans, sometimes dependent both on bioavailability and on microbial metabolism [21–23]. Some of the transporters involved in (poly)phenol bioavailability are also involved in SCFA absorption, giving rise to the possibility of interactions between these two classes in absorption and metabolism.

Hesperidin is the main (poly)phenol in sweet oranges. Due to an attached rutinose moiety, it passes through the small intestine unchanged to the colon [24], where combined activity of bacterial α-rhamnosidases and β-glucosidases release the aglycone hesperetin (HT) [25,26]. HT can be absorbed by passive transcellular diffusion, but its phase II metabolites are more hydrophilic and require active transport. Hesperetin-7-*O*-glucuronide (HT-7-glu), hesperetin-7-*O*-sulfate (HT-7-sul) and, to a lesser extent, hesperetin-3′-*O*-glucuronide (HT-3′-glu) interact with apically expressed ABCG2 while both glucuronides can interact with ABCC2 and basolateral ABCC3 [27,28]. Information on definitive interactions of HT-sul with efflux transporters is less convincing, possibly with efflux of HT-7-sul by ABCG2, but this remains debatable [27,29].

Hydroxycinnamic acids such as caffeic acid (in chlorogenic acid) are found in coffee and metabolized to ferulic acid (FA) in the colon. Similarly, FA in cereals and whole grain products is covalently bound to the indigestible cell wall polysaccharides *in planta* [30] and becomes bioaccessible only when released from the food matrix by esterase activity of the intestinal microbiota [31,32]. In intestinal cells, FA is partly absorbed *via* MCT1 and MCT4 [18,33] and undergoes glucuronidation by UGT1A1 isoforms [34]. Sulfation of FA by SULT1E1 and, to a lesser extent, by SULT1A1, an isoform particularly abundant in Caco-2 cells [34,35], has been previously reported. However, the exact transporters for FA conjugates are not yet known as ABCC2 (MRP2) and ABCG2 do not interact with phenolic sulfates or glucuronides [36].

To further our mechanistic understanding of the effect of SCFA on absorption of (poly)phenols, we used differentiated Caco-2 cell monolayers grown on permeable supports in a two-pronged approach: to investigate how long-term exposure of cells to SCFA and lactate could affect intestinal transformation and transport of two dietary gut-derived abundant bioactives (FA and HT) and to link this to changes in key shared transporters (MCT1, MCT4 and ABCG2) and detoxification systems (UGT1A) to explain the observed changes.

2. Materials and methods

2.1. Cell culture

Caco-2 cells were obtained from ATCC (ATCC-HTB37; LGC Standards, Teddington, Middlesex, UK) and maintained in Dulbecco's modified Eagle's medium containing 4.5 g/L glucose supplemented with 2% GlutaMAX (GIBCO, Life Technologies, Thermo Fisher Scientific, Paisley, UK), 1% nonessential amino acids, 1% sodium pyruvate, 1% penicillin/streptomycin and 10% heat-inactivated fetal bovine serum (FBS). Cells were kept in a humidified atmosphere at 37°C and 10% CO_2 in T75 flasks (Corning 430641; Appleton Woods, Birmingham, UK). Medium was changed every other day and cultures were passaged at 70–90% confluency using trypsin–EDTA (0.25%). All cell culture reagents were from Sigma (Sigma Aldrich, Gillingham, UK) unless otherwise stated.

2.2. Experimental conditions

Caco-2 cells were seeded on 6-well transwell dishes (Corning 3412; Appleton Woods, UK) at a density of 6×10^4 cm^{-2} and maintained for 21–23 days. From day 7 postseeding, the medium in the apical compartment was depleted of FBS and supplemented with a final concentration of 1 mM Na-acetate, Na-propionate, Na-butyrate or Na-lactate or an equimolar mixture of these four compounds (0.25 mM each, total concentration of 1 mM). FBS in the basal compartment medium was increased to 20% to mimic intestinal conditions. Stocks of SCFA were prepared in 25% DMSO resulting in a final concentration of 0.1% DMSO, which was used as control. High-purity (18.2 MΩ cm^{-1}) water supplied by a MilliQ system (Merck Millipore UK, Watford, UK) was used throughout this work.

2.3. Immunofluorescence

For immunostaining, Caco-2 cells were seeded on 12-well Millicell culture dishes (MCHT12H48; Merck Millipore) and allowed to grow as described in Section 2.2. After 21–23 days, cells were washed with ice-cold PBS, fixed with 4% paraformaldehyde in PBS for 15 min and incubated with fluorescein-labeled wheat germ agglutinin (Vector Laboratories, Peterborough, UK) for 10 min. Cells were permeabilized with 0.1% Triton X-100 and incubated with MCT1 (sc-365501; Santa Cruz Biotechnology, Insight Biotechnology, Middlesex, UK), MCT4 (sc-376139; Santa Cruz Biotechnology, Insight Biotechnology) or ABCG2 (NBP1-59749; Novus Antibodies, Bio-Techne, Cambridge, UK) antibodies at a dilution of 1:15 for MCT1 and MCT4 and 1:50 for ABCG2 for 1 h at room temperature. After washing with PBS, cells were further incubated with Cy3-conjugated donkey antimouse IgG (MCTs) or antirabbit IgG (ABCG2) (Jackson ImmunoResearch, West Grove, Pennsylvania, USA) at a 1:300 dilution. Nuclei were stained using 2 μg/ml DAPI and Millicell filters were removed with a scalpel and mounted on microscopy slides with ProLong Gold antifade reagent (Molecular Probes, Thermo Fisher Scientific, Paisley, UK). A similar protocol was followed for detection of tight junctions, using Claudin 1 rabbit antibody (ab180158; Abcam, Cambridge, UK) at 1:400 and Alexa488-conjugated antirabbit IgG (Jackson ImmunoResearch) at 1:300 dilution. Cell images were obtained with a Zeiss LSM700 inverted confocal microscope with a 63× (NA 1.4) or 40× (NA 1.3) objective.

2.4. Gene expression analysis by ddPCR

Caco-2 cells were seeded on 6-well transwell dishes and treated as described in Section 2.2. On days 21–23, cells were washed with ice-cold PBS, scraped from filters, and mRNA was extracted using the Ambion RNAqueous kit (AM1912; Ambion, Life Technologies, Thermo Fisher Scientific), according to the manufacturer's protocol. One microgram of RNA was transcribed to cDNA using the Applied Biosystems high-capacity RNA to cDNA kit (4387406; Life Technologies, Thermo Fisher Scientific). The QX100 Droplet Digital PCR system (ddPCR; BioRad Laboratories, Hercules, CA, USA) was used to quantify changes in gene expression of MCT1, MCT4 and ABCG2 from four biological replicates from two seeding experiments (total, $n=4$), with three technical replicates each. Each assay (20 μl) consisted of reaction mix prepared with 0.65 ng of transcribed cDNA diluted with MilliQ water to 9 μl; 1 μl of FAM-labeled TaqMan primer of MCT1, MCT4 or ABCG2; 1 μl of VIC-labeled TaqMan primer of TBP (TATA box binding protein) (all from Life Technologies, Thermo Fisher Scientific); and 10 μl ddPCR Supermix for Probes (No dUTP) (BioRad Laboratories UK, Hemel, Hertfordshire, UK). PCR mixture-containing droplets were generated according to manufacturer's guidelines with the QX100 droplet generator before cycling in a C1000 touch thermal cycler (BioRad Laboratories, Hercules, CA, USA) at optimal annealing/extension temperature for every primer. On average, ddPCR yielded 16,103±1148 (standard deviation) accepted droplets per well. Data from the QX100 Droplet Reader were analyzed with the QuantaSoft software (Kosice, Slovakia). Concentration of the target DNA in copies per microliter was calculated from the fraction of positive reactions using Poisson distribution analysis. Results shown represent total copies of each transporter and of TBP per nanogram of cDNA. All reactions were performed in duplex mode. The ddPCR data for each target gene are collected independently based on fluorescence signal and copy numbers are reported for all. Therefore, the housekeeping gene expression can be monitored but is not necessary for data evaluation. Although multiplexing with TBP was intended as a housekeeping gene, small changes in copy number were observed and these are also reported here. The Applied Biosystems ID of the primer/probe set for MCT1 (SLC16A1) was Hs00161826_m1, that for MCT4 (SLC16A3) was Hs00358829_m1, that for ABCG2 was Hs01053790_m1 and that for TBP was Hs00427620_m1.

2.5. Protein analysis — Simple Western immunoassays

For protein detection, Caco-2 cells were grown on 6-well transwell dishes as described in Section 2.2. At 21–23 days, cells were washed with ice-cold PBS, scraped and lysed in Bicine-CHAPS buffer (ProteinSimple, San Jose, CA, USA) containing 1% protease (P8340) and 1% phosphatase inhibitor cocktail (P0044 and P5762) (Sigma Aldrich). The lysate was centrifuged at 14,000*g* for 10 min at 4°C and the total protein concentration of the supernatant was determined by BCA microplate assay (Pierce Biotechnology, Thermo Fisher Scientific) according to manufacturer's instructions. MCT1, MCT4, ABCG2 and UGT1A protein abundance was determined using the ProteinSimple system "WES" (Bio-Techne, ProteinSimple) according to manufacturer's

instructions. For MCT1, MCT4 and UGT1A detection, samples were denatured by incubation with DTT and SDS-containing Master Mix (Bio-Techne, ProteinSimple) at 37°C for 20 min. Because of differences in compatibility of antibodies when multiplexing and denaturing condition requirements for the individual protein targets, different loading controls were tested and selected for each protein of interest. Claudin 1, a tight junction marker (1:50, mouse monoclonal, #37-4900; Invitrogen, Life Technologies, Thermo Fisher Scientific) was used as a loading control and run in the same capillary as MCT1 (1:25, mouse monoclonal, sc-365501; Santa Cruz Biotechnology, Insight Biotechnology) and MCT4 (1:25, mouse monoclonal, sc-376139; Santa Cruz Biotechnology, Insight Biotechnology). For ABCG2 determination, α-tubulin (1:50, rabbit monoclonal, 2125S; Cell Signalling Technology, New England Biolabs, Hertfordshire, UK) was used as a loading control and detected from the same sample run in separate capillaries (1:50, rabbit polyclonal NBP1-59749; Novus Antibodies, Bio-Techne). Denaturation was carried out by incubation for 5 min at 95°C. Claudin 1 (1:50, rabbit monoclonal, ab180158; Abcam, Cambridge, UK) was also used as loading control for UGT1A (1:50, rabbit polyclonal, sc-25847; Santa Cruz Biotechnology, Insight Biotechnology) and both run in the same capillary. All antibodies were used in the linear response range following optimization (Fig. A.3). Quantification of peak areas and gel image reconstruction was carried out using the ProteinSimple Compass software. Every sample including the biotinylated ladder contained three fluorescent molecular weight standards that were used to align each individual capillary with the ladder and assign the molecular weights to detected peaks.

2.6. Transport experiments

For transport experiments, Caco-2 cells were grown on 6-well transwell dishes as described in Section 2.2. At 21–23 days, cells were washed twice with Hank's Balanced Salt Solution (HBSS) containing 1.8 mM $CaCl_2$ at pH 7.4 and allowed to equilibrate for 30 min in a humidified atmosphere at 37°C and 10% CO_2. Monolayer integrity was determined by the Transepithelial Electrical Resistance (TEER) of the cell layer measured with the Millicell ERS voltohmmeter (Merck Millipore UK) and, at the same stage, cell differentiation was also confirmed by Claudin 1 staining of tight junctions in separately seeded dishes (Fig. A.2). Monolayers with a TEER value lower than 930 Ω cm^2 were discarded. HBSS was aspirated and 2 ml fresh HBSS was added to the basal compartment for the transport experiment. In the apical compartment, 2 ml HBSS containing 20 μM HT, 500 μM FA or 1 mM salicylic acid (SA) was added. SA was used as a positive control for MCT-dependent transport [37]. After 30 min (SA) or 1 h (HT or FA) incubation, TEER values were measured again to confirm sustained monolayer integrity. Incubation times were chosen according to previous transport experiments reported in the literature for these compounds. A total of 500 μl aliquots of media were collected from both compartments and ascorbic acid was added to 100 μM. Samples were then stored at −80°C until further analysis.

2.7. LC-MS/MS analysis

HT and FA metabolites were analyzed by high-performance liquid chromatography (HPLC) mass spectrometry. Separation was carried out on a Phenomenex Kinetex XB C18, 2.1×100 mm, 2.6 μm column (Phenomenex, Cheshire, UK) set to 35°C. Solvent A was 5% acetonitrile in MilliQ water containing 0.1% formic acid, and solvent B was 5% MilliQ water in acetonitrile containing 0.1% formic acid. All solvents were of mass spectrometry grade (VWR, Leicestershire, UK). Flow rate was 0.25 ml/min, and injection volume was 10 μl. The HPLC system (Agilent 1200 series; Agilent Technologies, Waldbronn, Germany) was coupled to an Agilent 6410 ESI-MS/MS (Agilent Technologies, Santa Clara, CA, USA) set to negative ion mode and multiple reaction monitoring (MRM) scanning was applied to quantify compounds. Fragmentor voltages and collision energies were optimized for each compound using pure standard solutions.

Daidzein, 3,4-dimethoxycinnamic acid (DMCA), ascorbic acid, dihydroferulic acid (DHFA), HT and FA were purchased from Sigma (Sigma Aldrich). Ferulic acid-4-*O*-sulfate (FA-sul) was synthesized by Dr. Nicolai U. Kraut (University of Leeds, Leeds, UK), FA and HT glucuronides were kindly provided by Prof. Denis Barron (Nestlé Institute of Health Sciences, Lausanne, Switzerland) and hesperetin-3′-*O*-sulfate (HT-3′-sul) was a gift from Dr. Christine Morand (INRA, Human Nutrition Unit, France). Quantification was based on a 6-level matrix matched calibration and peak areas were normalized to the peak area of the internal standard.

For the analysis of HT metabolites, samples were thawed and an aliquot of 510 μl was mixed with 500 μl methanol containing 20 μM daidzein as internal standard. Compounds were eluted with the following gradient: 0–22 min, isocratic on 12% B; 22–32 min linear from 12% to 35% B; 32–33 min linear from 35% to 90% B; 33–35 min isocratic on 90% B; 35–36 min linear from 90% to 12% B and 36–50 min isocratic on 12% B. The following MRM transition pairs were used for identification: HT, 301→151; HT glucuronides, 477→301; HT sulfates, 381→301 and daidzein, 253→133. Concentrations of HT-7-sul were estimated based on the response factor of HT-3′-sul and results are expressed as HT-3′-sul equivalents.

For the analysis of FA metabolites, samples were thawed and acetic acid and internal standard DMCA were added to 510 μl of sample to a final concentration of 10 mM and 10 μM, respectively. Samples were analyzed as above, except that the gradient used for elution was 0–1 min: isocratic on 5% B, 1–10 min linear from 5% to 35% B, 10–11 min linear from 35% to 90% B, 11–13 min isocratic on 90% B, 13–14 min linear from 90% to 5% B and 14–30 min isocratic on 5% B. Set MRM transitions used were as follows: for FA, 193→134; for DHFA, 195→136; for FA-sul, 273→193; for FA-glu, 369→193 and for DMCA, 207→103.

For SA transport, apical and basolateral samples were analyzed on an HPLC-UV (Agilent 1200 series) system. An Agilent XDB-C18, 4.6×100 mm, 1.8 μm column (Agilent Technologies, Cheshire, UK) with a flow rate of 0.6 ml/min, injection volume of 5 μl and a 3-min-long isocratic elution at 35% B. The peak areas determined at 303 nm and at 326 nm were utilized to quantify SA and the DMCA internal standard by comparison to original standards. Samples for SA analysis were prepared in the same way as for the FA metabolites. All samples were centrifuged at 17,000*g* for 5 min before injection.

2.8. Data analysis

For transport experiments, all results are presented as mean values of six biological replicates analyzed in duplicate and error bars indicate the standard error of the mean (S.E.M.). Statistical analysis was performed using *R* and independent samples Student's *t* test. Results were considered of statistical significance when $P<.01$. For changes in gene expression and protein analysis, values shown are the mean of three to six biological replicates ±S.E.M., as indicated in the figure legends. For analysis of statistical significance, independent samples Student's *t* test was employed and analysis was carried out with SPSS Statistics (v22, IBM).

3. Results

3.1. Transport of metabolites across Caco-2 cell monolayers

We investigated the chronic effect (14 days) of butyrate, propionate, acetate, lactate or their equimolar mixture on the transport and metabolism of HT (Fig. 1), FA (Fig. 2) and SA (Fig. 3) in differentiated Caco-2 cells. Tight junction integrity of untreated cells was confirmed both by TEER measurement and Claudin 1 staining, indicating uniform monolayers (Fig. A.2). Compared to untreated cells, butyrate pretreatment decreased average TEER values by 7% from 1149±23 Ω cm^2 to 1066±31 Ω cm^2 ($n=36$, $P<.001$), whereas lactate increased the resistance by 7% to 1232±25 Ω cm^2 ($n=36$, $P=.002$). During the transport experiment, all average TEER values remained higher than 930 Ω cm^2, confirming monolayer integrity [33].

HT and its metabolites were measured relative to authentic standards in the apical and basolateral compartments. From representative chromatograms (Fig. A.1), it is apparent that two isomers of HT-3′-glu were present in the original standard. These are annotated as HT-3′-glu 1 and HT-3′-glu 2, corresponding to presumed *R* and *S* enantiomers, and the sum of the two peaks was used. In cells not treated with SCFA, some HT was transported unchanged through the cells to the basolateral compartment (87±26 pmol/min), representing 13% of HT added apically after 60 min incubation. The main phase II metabolite formed was HT-7-glu, present both in the basal (12.33± 0.57 pmol/min) and apical (3.87±0.07 pmol/min) compartments accounting in total for 2.4% of the original HT added apically. For HT-3′-glu, the total rate of transport of HT-3′-glu 1 and HT-3′-glu 2 to the basolateral side was approximately 3-fold higher than efflux to the apical side.

Butyrate treatment increased HT-7-glu levels apically by 12% and by 23% in the basal compartment, whereas the formation of HT-3′-glu 2 was decreased by 30–40% ($n=6$, $P<.01$). Following propionate treatment, a higher rate of glucuronidation of HT was evidenced; HT-3′-glu 1 increased by 52% and HT-7-glu increased by 32%, while in the basolateral side, HT-7-glu and HT-3′-glu 1 were 42% and 34% higher, respectively ($n=6$, $P<.01$). In comparison, acetate decreased the production of HT-3′-glu 2 by 20% ($n=6$, $P<.01$) in both compartments. All HT phase II conjugates were 13–40% lower in the apical compartment following lactate treatment, and HT-3′-glu 1 and HT-3′-glu 2 were also substantially decreased in the basolateral side ($n=6$, $P<.01$). Transport of sulfated HT conjugates to apical and basal compartments was comparable in untreated cells, with 1.9±0.03 and 2.53±0.06 pmol/min in the basal and 2.6±0.06 and 2.8±0.1 pmol/min in the apical compartments, for the 7 and 3′ conjugates, respectively (Fig. 1). HT-3′-sul efflux to the apical direction was

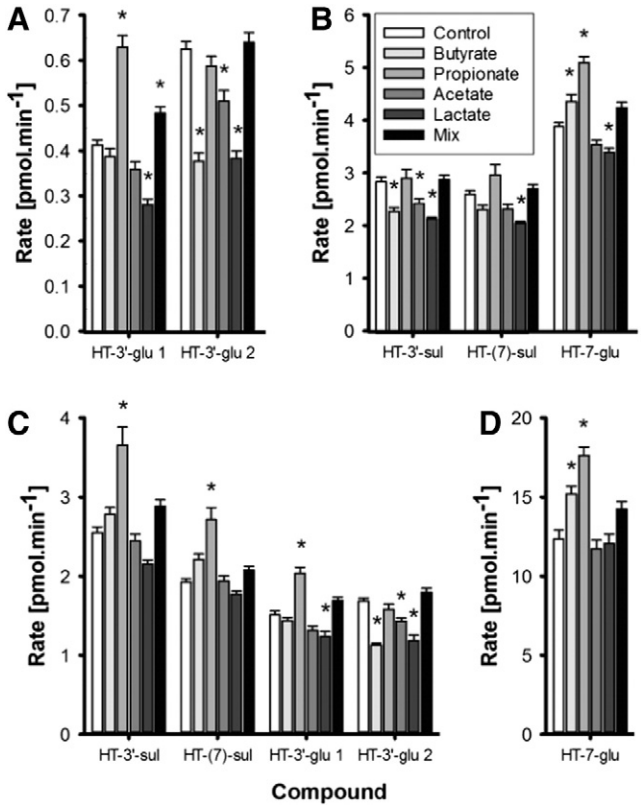

Fig. 1. Transport of HT phase II conjugates in the apical (A and B) and basolateral (C and D) compartments in Caco-2 cells following treatment with 1 mM individual SCFA, lactate or a mix for 14 days and incubation with 40 nmol of HT added to the apical compartment (n=6) for 1 h. Statistically significant changes in the concentration of HT conjugates are indicated (*) when compared to control cells (Control) without treatment (P<.01).

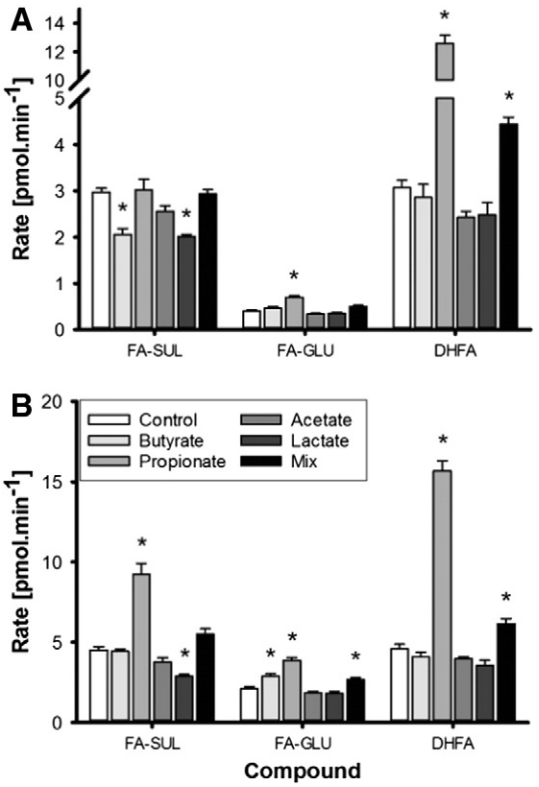

Fig. 2. Transport of FA phase II conjugates in the apical (A) and basolateral (B) compartments in Caco-2 cells following treatment with 1 mM individual SCFA, lactate or a mix for 14 days and incubation with 1 μmol of FA added to the apical compartment (n=6) for 1 h. Statistically significant changes in the concentration of HT conjugates are indicated (*) when compared to control cells (Control) without treatment (P<.01).

lower with butyrate, acetate and lactate treatments while both HT-3′-sul and HT-7-sul basolateral transport were stimulated by propionate treatment. When an equimolar mixture of acetate, propionate, butyrate and lactate was used, efflux of HT-3′-glu 1 to the apical side was increased.

After incubation of FA with Caco-2 monolayers, some FA was transported (1.73±0.17 nmol/min) to the basal compartment accounting for 10.4% of added FA after 1 h. Metabolites were preferentially transported towards the basal side, with the most abundant being DHFA and FA-sul (Fig. 2). FA-sul was lower apically after butyrate treatment, while FA-glu increased by ~40%, but only in the basal compartment (n=6, P<.01). In comparison, propionate treatment increased FA-glu equally in both sides, by 72% in the apical and 83% in the basolateral. Conversion of FA into DHFA was also strongly stimulated, resulting in 3.4-fold (n=6, P<.001) and 4.1-fold higher concentration of DHFA in the basal and apical compartments, respectively (n=6, P<.001), while transport of sulfate conjugates to the basolateral side was favored over efflux to the apical compartment. Acetate had no effect on FA transport and metabolism, while FA-sul substantially decreased in both compartments (n=6, P<.01) following lactate treatment. A mixture of acetate, propionate, butyrate and lactate led to an increase in FA-glu on the basal side, while DHFA concentrations were higher in both compartments (n=6, P<.01). The latter effect was comparable to the effect of propionate treatment alone.

Transport of SA to the basolateral side was quite efficient when compared to HT and FA or their metabolites and accounted for ~10% of the original amount added apically within 30 min (Fig. 3). SA transport was stimulated by butyrate and propionate resulting in a 32% and 21% increase in the basolateral compartment compared to untreated cells (n=6, P=.003), while acetate and lactate did not affect SA transport.

3.2. Effect of acetate, propionate, butyrate and lactate on transporters and UGT1A expression

MCT1 and MCT4 are involved in the transport of SA and FA, whereas ABCG2 transports HT conjugates. Cellular localization of these transporters was confirmed in our model by indirect immunofluorescent staining (Fig. A.2). ABCG2 was mainly present at the apical membrane but also detected in the lateral membrane and in the nucleus. MCT1 was evident on the apical and lateral membranes and the nuclear envelope, while MCT4 was specifically located in the lateral and basal membranes, in agreement with previous studies. Changes in MCT1, MCT4 and ABCG2 mRNA after treatment with SCFA or lactate are shown in Fig. 4. Concomitant changes in MCT1, MCT4, ABCG2 and UGT protein are shown in Fig. 5. To ensure true quantification of these specific proteins, all of the antibodies used were evaluated for linearity and specificity alone and when multiplexed and only used within the validated linear range (Fig. A.3). No significant changes were found in reference loading proteins under the experimental conditions (Fig. 5).

Butyrate treatment decreased MCT1 mRNA by ~30% (n=4, P<.005) while MCT1 protein was increased by ~40% (n=3, P=.01). MCT4 mRNA and protein levels were not affected by butyrate, and although ABCG2 mRNA decreased (n=4, P<.005), this was not reflected in

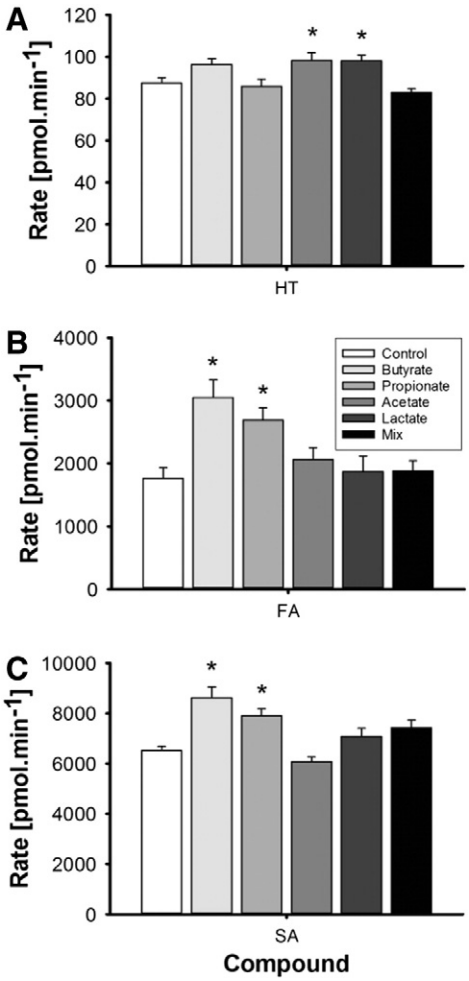

Fig. 3. Transport of HT (A), FA (B) and SA (C) by Caco-2 cells to the basolateral compartment. Cells were treated with 1 mM of SCFA, lactate or a mix for 14 days followed by the transport experiment. Statistically significant changes in concentrations are indicated (*) when compared to control cells (Control) without treatment ($P<.01$).

protein changes. In comparison, following treatment with propionate for 14 days, gene expression of MCT1 was unchanged whereas MCT4 was increased by ~29% ($n=4$, $P<.005$) without significant effects on MCT1 and MCT4 protein levels. However, both ABCG2 mRNA and protein levels were lower by ~18% and ~40% respectively ($P<.01$), following chronic propionate exposure. Acetate increased MCT1 ($n=4$, $P\leq.02$) and MCT4 ($n=4$, $P\leq.005$) mRNA levels by ~20%, while ABCG2 mRNA was unaffected; MCT1 protein was decreased by ~30% ($n=3$, $P<.005$) and UGT1A by ~25% ($n=4$, $P=.02$), while MCT4 and ABCG2 were similar to basal levels. Following 14 days of lactate treatment, MCT1, MCT4 and ABCG2 gene expression was lower by ~20–30% ($P<.001$) while ABCG2 and UGT1A protein levels were ~50% ($n=3$, $P=.005$) and ~30% lower ($n=3$, $P=.009$), respectively. An equimolar mixture of all SCFA and lactate led to 37% higher MCT4 mRNA ($n=4$, $P<.001$) and 14% lower ABCG2 mRNA ($n=4$, $P<.001$), but these changes were not reflected at the protein level.

4. Discussion

The Caco-2 cell line, when grown on a permeable support, displays morphological and biochemical properties of intestinal enterocytes and expresses drug transporting enzymes simulating the intestinal membrane barrier [38]. To mimic the *in vivo* gut maturation process, we have used a long-term treatment approach during the differentiation stage. We investigated SCFA-induced changes in transport and metabolism of two abundant microbial metabolites of dietary (poly)phenols, HT and FA, and we linked these to changes in transporter and UGT mRNA and protein to explain the mechanism of the metabolic changes. The multiple interactions observed are complex and are summarized in Fig. 6. Butyrate is considered a beneficial fermentation product of dietary fiber, and part of the benefit may derive from its ability to chronically increase the uptake of hesperetin glucuronide, decreasing efflux of (poly)phenol conjugates back to the gut lumen and increasing uptake of phenolic acids through up-regulation of the MCT1 transporter.

Chronic butyrate and propionate treatment increased efflux of HT-7-glu to both compartments, in contrast to a decrease following acetate treatment. As changes were observed in both compartments, we hypothesized an effect on total glucuronidation of HT rather than transporters that are mostly direction specific; in Caco-2 cells, the enzymes involved are UGT1A1 and UGT1A3 [39]. Acetate treatment led to 25% lower UGT1A levels in agreement with transport data; however, butyrate and propionate treatment did not affect UGT1A. This could be due to a concomitant down-regulation of other UGT1A isoforms, for example, UGT1A7, 8 or 9, which are responsible for glucuronidation of HT at the 3′-OH [39], as is the case upon butyrate treatment. Because of sequence homology and complex posttranscriptional processing, antibodies for individual UGT1A family members are not commercially available, restricting investigation of individual isoforms. Both HT-3′-glu isomers identified here have been successfully separated by HPLC previously [39,40] and shown to have similar phase II metabolism efficiencies upon incubation of HT with human intestinal microsomes [39], in agreement with our results in the Caco-2 cell model. Propionate treatment specifically stimulated glucuronidation of HT-3′-glu 1, indicating that different enzymes may be involved in the conjugation to form different isomers.

Apical efflux of HT-7-glu is mediated by ABCG2 and, to a lesser extent, by ABCC2 (MRP2) [27,28]. Both chronic propionate and lactate treatments down-regulated ABCG2 protein expression, while only lactate had a significant effect on the apical efflux of HT-7-glu, leading us to speculate involvement of another apically located transporter such as ABCC2. Our hypothesis is further supported by lower apical efflux of both HT-3′-glucuronides upon lactate exposure, since HT-3′-glu interacts with ABCC2 but lacks affinity for ABCG2 [28].

Lactate also decreased apical efflux of both HT sulfates. Reports on the involvement of ABCG2 on HT-sul transport are inconsistent [27,29]. Because of apical localization of ABCG2, decreased protein expression can result in both lower apical efflux of substrates, as we observed for HT sulfates, or increased transport to the basolateral compartment, as seen for propionate-treated cells. Our results support a role of ABCG2 in HT-sul transport; however, other transporters cannot be excluded since both butyrate and acetate treatments also affected apical efflux without an effect on ABCG2.

FA and SA are partially taken up into the cell by apically located MCT1. Propionate and butyrate strongly enhanced transport of both compounds, while butyrate increased MCT1 protein, in agreement with previous work [37]. Basolateral efflux of these compounds is by MCT4, but under our experimental conditions, we did not observe significant changes in the regulation of MCT4. Differences in the experimental setup could explain this as previously butyrate supplementation was done for 22 days directly after seeding and on both apical and basolateral sides [37], which would enhance any observed effects. In our current experiments, SCFA were added for 14 days to confluent monolayers, and only apically, reflecting more closely the conditions *in vivo*.

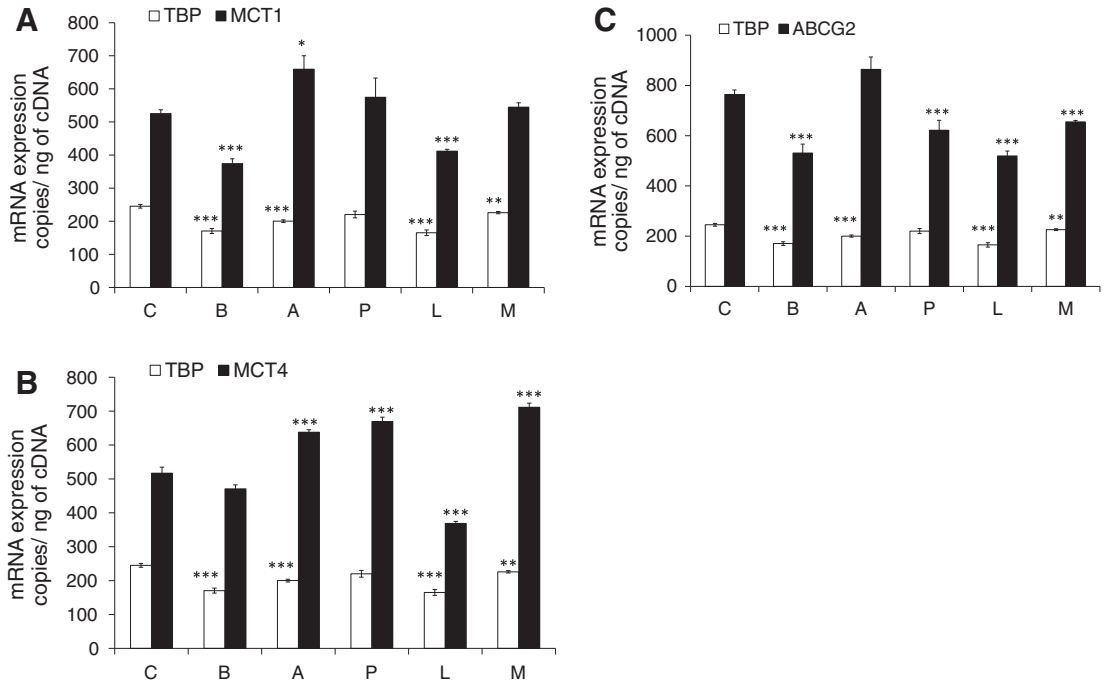

Fig. 4. mRNA expression of MCT1 (A), MCT4 (B) and ABCG2 (C) in differentiated Caco-2 cells following a 14-day treatment with 1 mM SCFA and lactate measured by ddPCR. Exact copy numbers of each transporter are shown per nanogram of cDNA. Four biological replicates from two experiments were analyzed in triplicate. TBP was multiplexed with each transporter as housekeeping gene but changes were also observed for TBP copy numbers. Statistically significant changes are indicated when compared to control cells (Control) without treatment (*P≤.02, **P≤.01, ***P≤.005). Error bars represent S.E.M. C, control; B, butyrate; A, acetate; P, propionate; L, lactate; M, mix.

Following cellular uptake, FA can be reduced to DHFA, and reductase activity is strongly stimulated by propionate. In accordance, the propionate and the mixed SCFA treatments resulted in higher quantities of DHFA, which can either passively diffuse extracellularly or be actively transported [41]. Glucuronidation of FA is also mediated by UGT1A isoforms [34,42]. Based on the transport results, we propose that propionate stimulates the activity of this enzyme, given the unilateral increase of FA-glu concentrations. UGT1A protein levels remained unchanged; however, any modest changes could be masked by the fact that the UGT1A antibody epitopes are raised in an overlapping area for all UGT1A isoforms as discussed above.

Hydroxycinnamic acids such as FA and their phase II metabolites were previously found not to interact with ABCG2 or ABCC2 [36]. Inhibition of MRPs previously resulted in decreased transport of FA-glu and DHFA to the basolateral compartment [41]. ABCC3 (MRP3) and ABCC6 (MRP6) were suggested as possible candidates [41,43,44]. In intestinal cells, sulfation of FA to FA-4-*O*-sulfate occurs *via* SULT1E1 or SULT1A1 activity [34]. Here, butyrate decreased apical efflux of FA-sul, and propionate augmented transport of FA-sul to the basolateral compartment.

Mechanistic data regarding effects of SCFA or lactate on phase II metabolism were previously very limited [18]. Other physiological changes caused by SCFA are known to be mediated through interaction with G-protein-coupled receptors or inhibition of histone deacetylases [45–47]. For example, in this work, TBP gene expression, a target of histone deacetylases, was consistently down-regulated with all SCFA treatments pointing to such a possible mechanism. SCFA can also modulate expression of conjugating enzymes through PPAR activation [48,49]. Many endogenous compounds are also known to modulate UGT and SULT expression by specifically targeting members of the nuclear receptor superfamily to which PPAR belongs [50–54]. These interactions are clearly complex especially since colonocytes are exposed to high but varying concentrations of SCFA and lactate *in vivo*, which would lead to constantly changing effects on (poly)phenol absorption and metabolism, depending on dietary composition.

Overall, propionate and butyrate stimulated the transport and phase II metabolism of HT, FA and SA, resulting in increased bioavailability in Caco-2 cells. *In vivo*, consumption of a diet rich in prebiotics can increase propionate and butyrate production by the colonic microbiota while decreasing acetate and lactate, thereby enhancing (poly)phenol bioavailability and reinforcing alleged beneficial effects on gut health. For example, prebiotic fibers such as inulin shifted the relative contributions of acetate: propionate: butyrate from 65:23:12 to 43:37:20 while brown rice also changed the relative amounts of the same SCFA in pigs from 68:26:6 to 62:33:5 compared to white rice consumption [5,55]. Besides fiber, (poly)phenols can themselves act as prebiotics, for example, by inhibiting α-amylase activity resulting in more resistant starch in the colon [56].

By exposing Caco-2 cells chronically to different SCFAs during the differentiation phase, we have shown how they may affect (poly)phenol bioavailability. Most certainly, these results emphasize that the microbiome and diet interactions will remain a key component of the 21st century pharmacopoeia, as it provides a modifier, target and source for the bioactive components, natural or synthetic, of the future [1].

Conflict of interest

This work received partial funding by a STSM grant by INFOGEST (COST FA 1005) to EVR. GW has recently received other research funding from Florida Department of Citrus, USA, and conducted consultancy for Nutrilite, USA, and Suntory, UK.

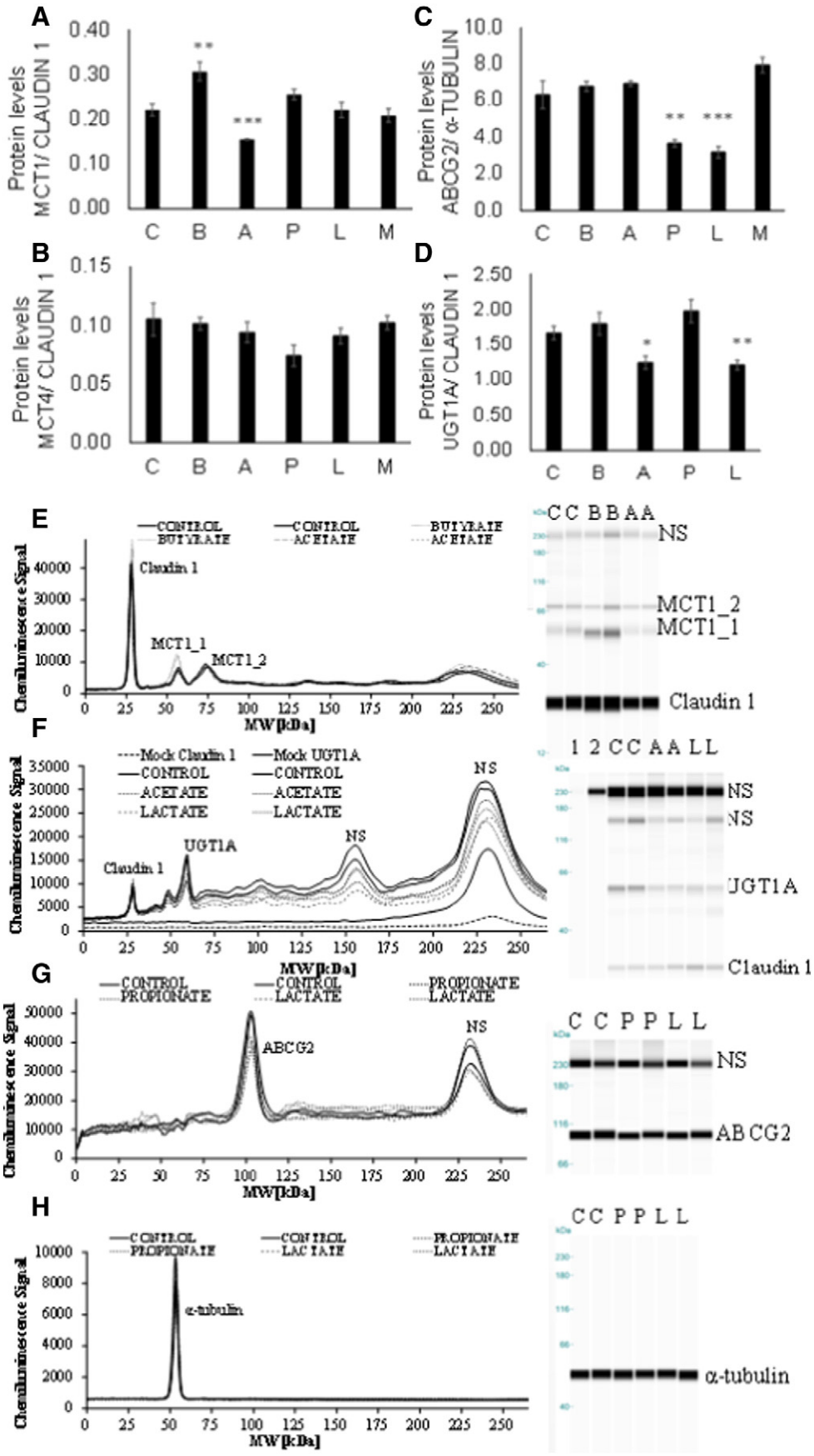
A
Protein levels MCT1/ CLAUDIN 1
0.40
0.30
0.20
0.10
0.00
**
***
C B A P L M
C
Protein levels ABCG2/ α-TUBULIN
10.0
8.0
6.0
4.0
2.0
0.0
**
***
C B A P L M
B
Protein levels MCT4/ CLAUDIN 1
0.15
0.10
0.05
0.00
C B A P L M
D
Protein levels UGT1A/ CLAUDIN 1
2.50
2.00
1.50
1.00
0.50
0.00
*
**
C B A P L
E
CONTROL
BUTYRATE
CONTROL
ACETATE
BUTYRATE
ACETATE
Chemiluminescence Signal
40000
30000
20000
10000
0
Claudin 1
MCT1_1
MCT1_2
0 25 50 75 100 125 150 175 200 225 250
MW[kDa]
C C B B A A
NS
MCT1_2
MCT1_1
Claudin 1
F
Mock Claudin 1
CONTROL
ACETATE
LACTATE
Mock UGT1A
CONTROL
ACETATE
LACTATE
Chemiluminescence Signal
35000
30000
25000
20000
15000
10000
5000
0
Claudin 1
UGT1A
NS
NS
0 25 50 75 100 125 150 175 200 225 250
MW[kDa]
1 2 C C A A L L
NS
NS
UGT1A
Claudin 1
G
CONTROL
PROPIONATE
CONTROL
LACTATE
PROPIONATE
LACTATE
Chemiluminescence Signal
50000
40000
30000
20000
10000
0
ABCG2
NS
0 25 50 75 100 125 150 175 200 225 250
MW[kDa]
C C P P L L
NS
ABCG2
H
CONTROL
PROPIONATE
CONTROL
LACTATE
PROPIONATE
LACTATE
Chemiluminescence Signal
10000
8000
6000
4000
2000
0
α-tubulin
0 25 50 75 100 125 150 175 200 225 250
MW[kDa]
C C P P L L
α-tubulin

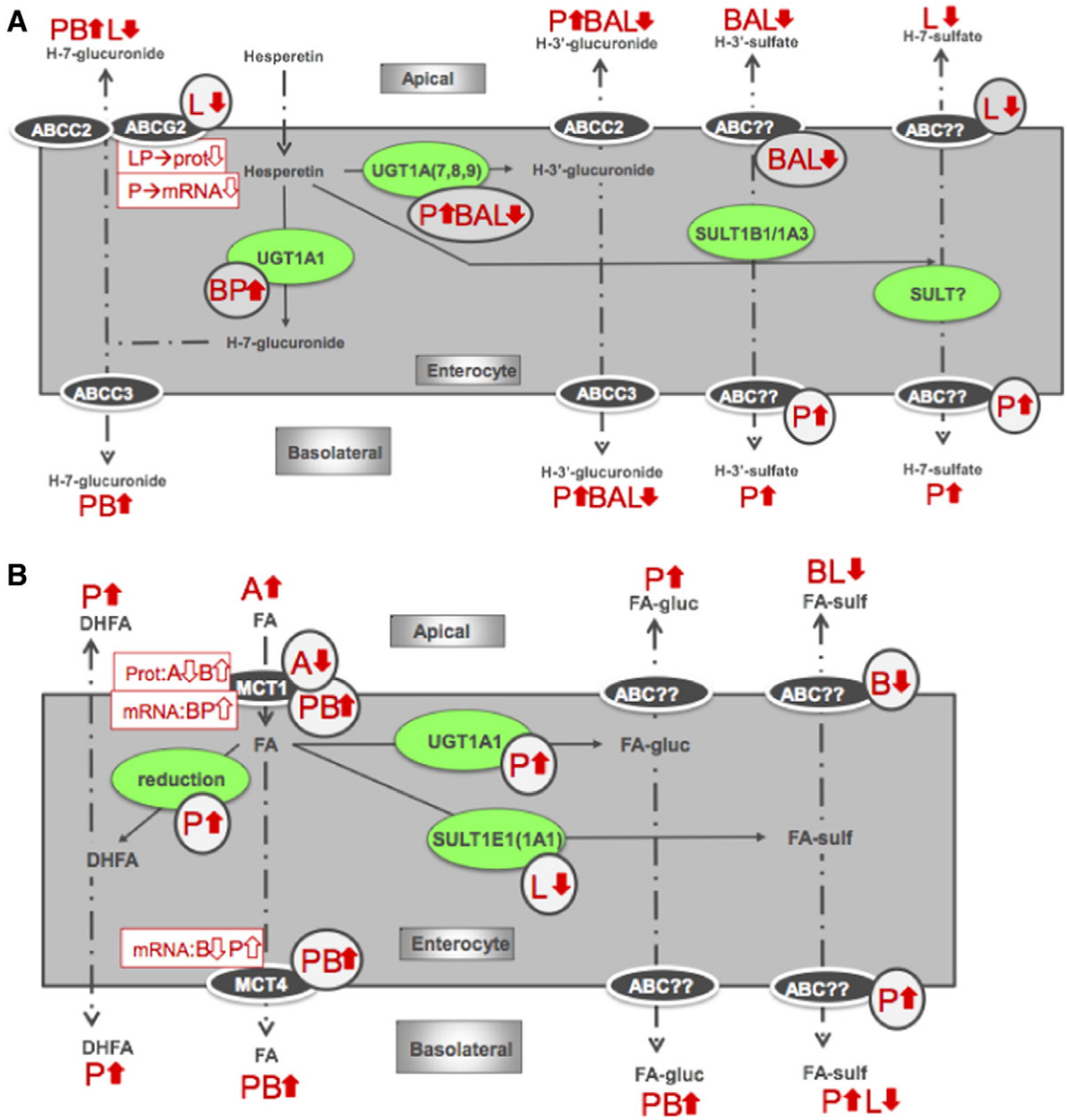

Fig. 6. Summary of HT (A) and FA (B) transport and conjugation in Caco-2 cells. A, acetate; P, propionate; B, butyrate; L, lactate. Changes in measured metabolite levels are indicated by thick arrows, circled arrows indicate predicted changes in enzymes or transporters and rectangular boxes indicate measured changes in mRNA or protein. Solid lines indicate metabolic changes; dot-dash lines indicate changes in localization of a metabolite.

Author contributions

AK and GW designed the study. EVR conducted transport experiments, AK and EVR performed gene and protein expression analysis, EVR and ST carried out immunostaining and LA and EVR carried out the LC-MS analysis. EVR, GW, LA, ST and AK interpreted and analyzed data. CG and JVC contributed essential materials and expertise. EVR wrote the first draft and all authors contributed to the final manuscript.

Acknowledgements

EVR is supported by the Agency for Innovation by Science and Technology in Flanders (IWT). The research leading to these results has received funding from the European Union Seventh Framework Program (FP7/2007-2013) under grant agreement number 312090 (BACCHUS) and European Research Council Advanced grant agreement number 322467 ("POLYTRUE?").

Fig. 5. Protein content of MCT1 (A), MCT4 (B), ABCG2 (C) and UGT1A (D) in Caco-2 cells measured by ProteinSimple WES. All antibodies were used in the linear response range following optimization (Fig. A.3). Pherogram and gel blot (lane) image view of duplicate representative samples are shown for treatments where significant changes were found (E–H). NS denotes nonspecific interactions of the antibodies with the fluorescence standards used in the ProteinSimple WES system. A representative view of such interactions (NS) is shown for UGT1A and Claudin 1 antibodies when run in separate lanes with all other components apart from sample [F: mock Claudin 1, mock UGT1A and (in F) in-gel blot image view; lanes 1 and 2]. An initial concentration of 1 mg/ml of Caco-2 whole cell lysate was used for MCT1 and MCT4 detection (A and B), 0.5 mg/ml for UGT1A (C) and 1.5 mg/ml for ABCG2 (and α-tubulin) (D). Statistically significant changes are indicated when compared to control cells (Control) without treatment (*$P \leq .02$, **$P \leq .01$, ***$P \leq .005$). Error bars represent S.E.M. C, control; B, butyrate; A, acetate; P, propionate; L, lactate; M, mix.

Appendix A

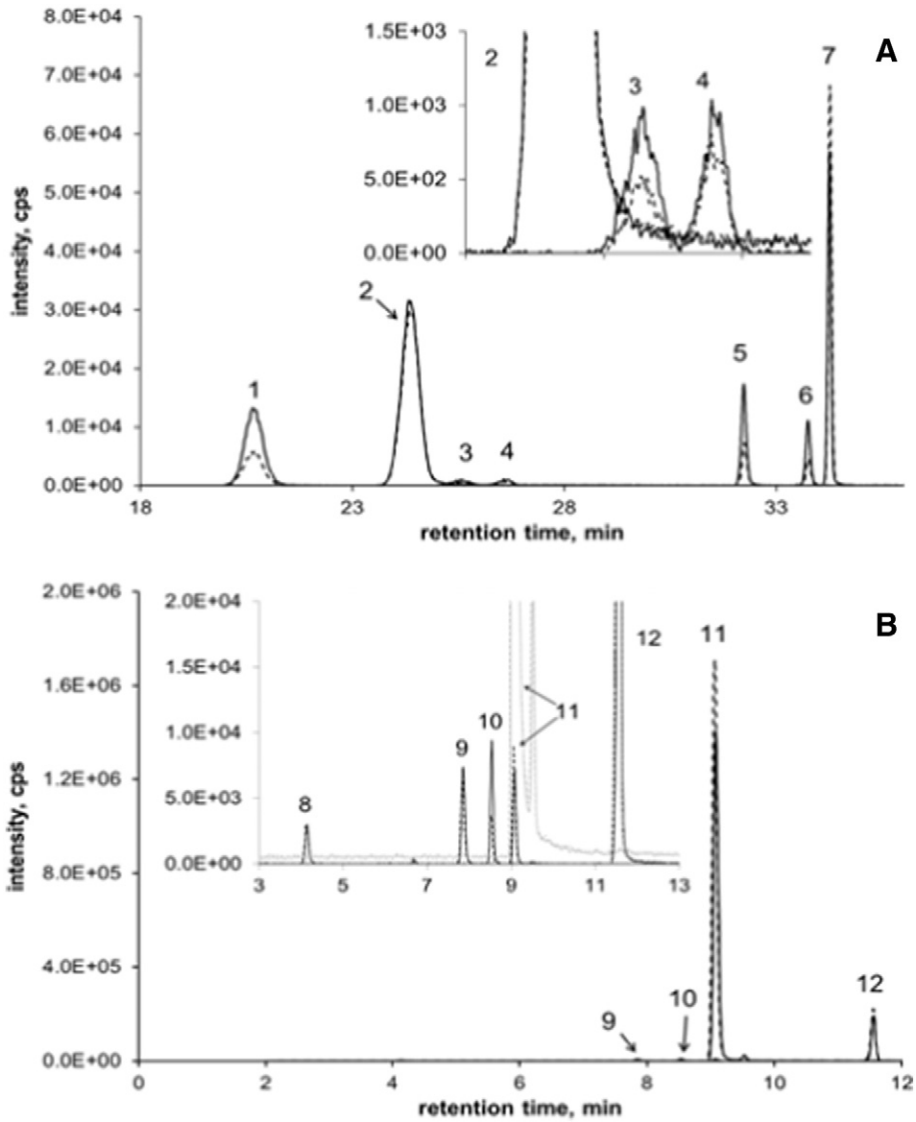

Fig. A.1. Representative chromatograms for HT (metabolites) (A) and FA (metabolites) (B). Dot-dash lines indicate samples and solid lines samples spiked with original standards for peak identification. 1: HT-7-glu, 2: daidzein (ISTD), 3 and 4: HT-3′-glu (assuming S, R), 5: HT-3′-sul, 6: HT-7-sul (qualitative identification, no standard), 7: HT, 8: FA-glu, 9: FA-sul, 10: DHFA, 11: FA and 12: 3,4-DMCA (ISTD).

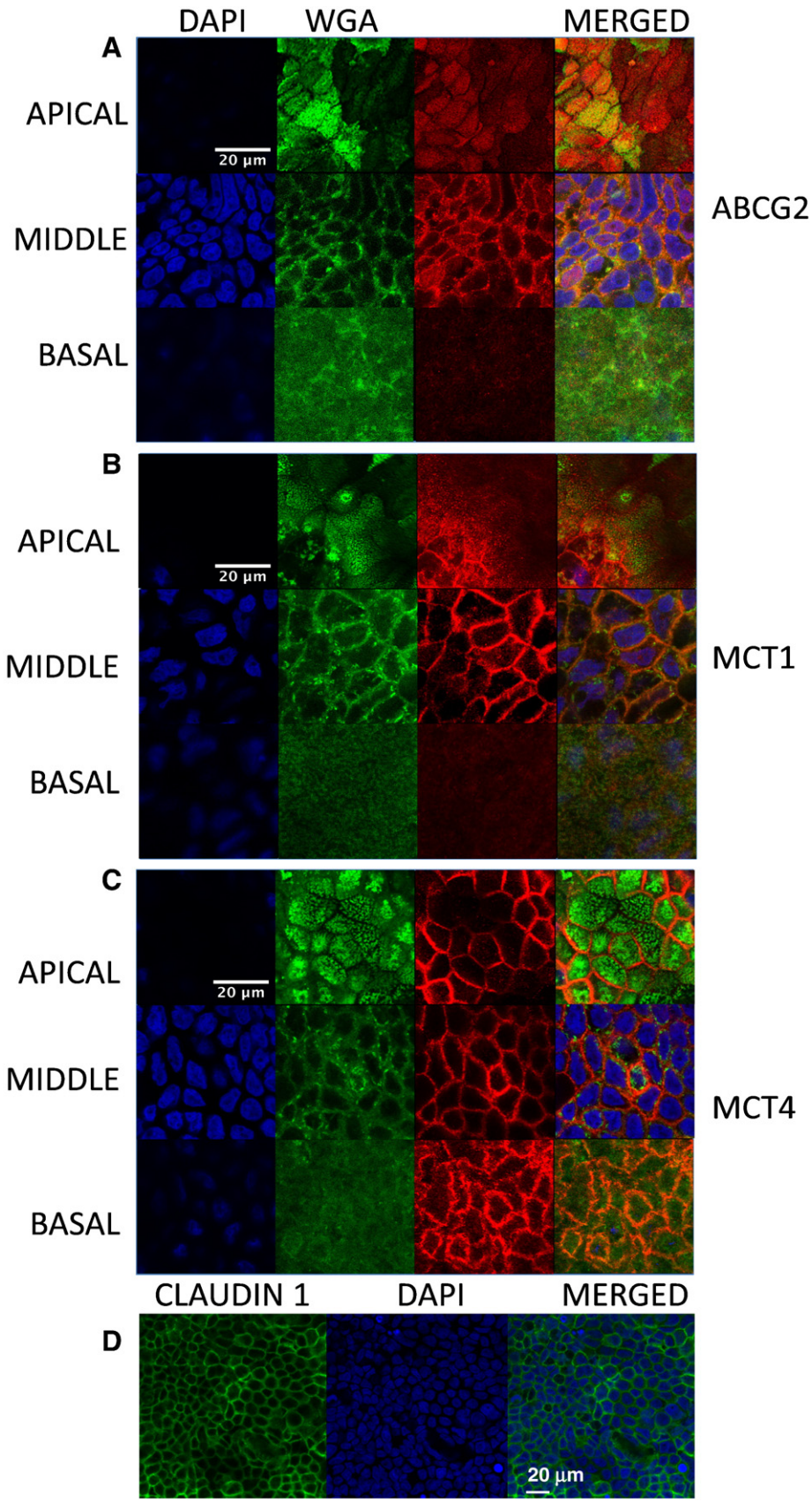

Fig. A.2. Indirect immunostaining of related transporters in differentiated Caco-2 cells. Cells were stained with DAPI (blue), membrane marker wheat germ agglutinin (WGA) (green) and anti-ABCG2 (A), anti-MCT1 (B) or anti-MCT4 (C) (red). Transporters appear orange when colocalizing with WGA and purple when colocalizing with DAPI. Tight junction formation immunostaining with Claudin 1 (D); cells were stained with DAPI (blue) and Claudin 1 (green).

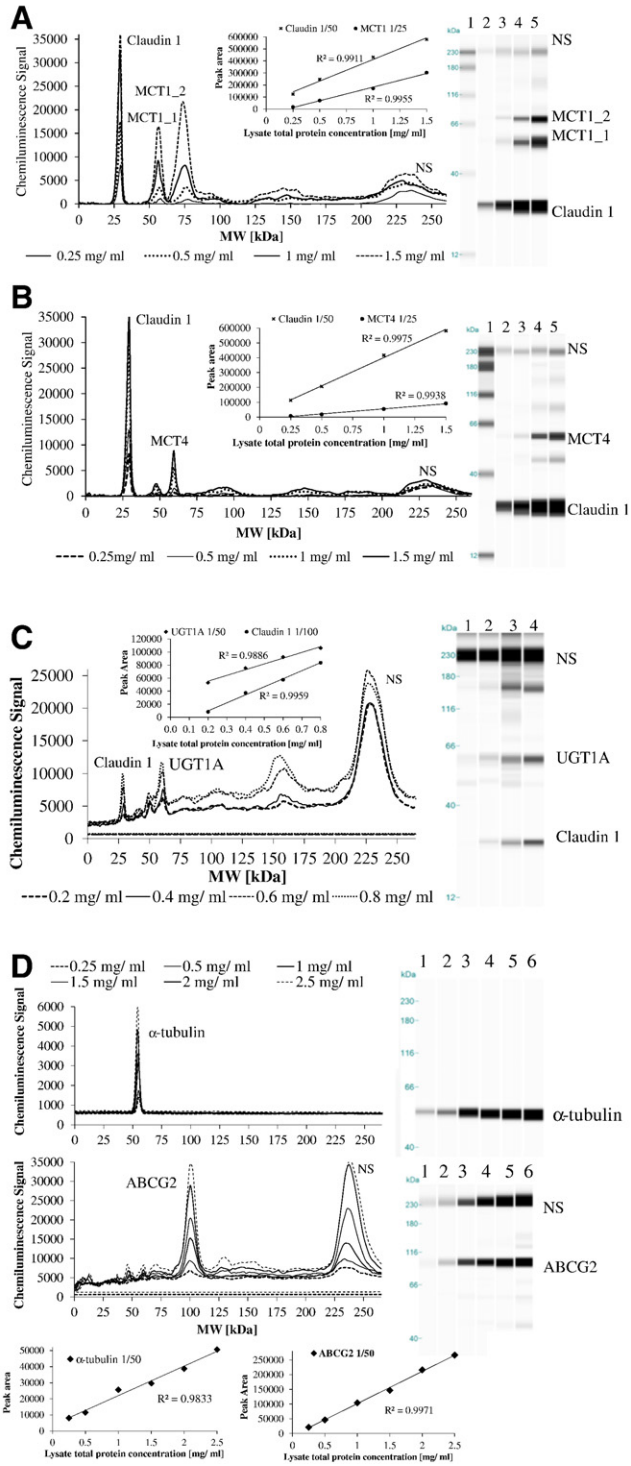

Fig. A.3. Protein detection by ProteinSimple WES system. Antibody validation for protein analysis of MCT1 (A), MCT4 (B), UGT1A (C) and ABCG2 (D). Images consist of pherogram view, gel blot image (lane view) corresponding to peaks and plotted standard curves indicating linearity of antibodies. Various amounts of total Caco-2 cell lysate were analyzed for the target and loading control proteins either in the same capillary [MCT1 (A), MCT4 (B) or UGT1A (C)] or separate capillaries [ABCG2 (D)]. NS denotes nonspecific interactions of the antibodies with the fluorescence standards used in the ProteinSimple WES system.

References

[1] Spanogiannopoulos P, Bess EN, Carmody RN, Turnbaugh PJ. The microbial pharmacists within us: a metagenomic view of xenobiotic metabolism. Nat Rev Microbiol 2016;14(5):273–87. http://dx.doi.org/10.1038/nrmicro.2016.17.

[2] Pryde SE, Duncan SH, Hold GL, Stewart CS, Flint HJ. The microbiology of butyrate formation in the human colon. FEMS Microbiol Lett 2002;217:133–9.

[3] Wong JMW, de Souza R, Kendall CWC, Emam A, Jenkins DJA. Colonic health: fermentation and short chain fatty acids. J Clin Gastroenterol 2006;40:235–43. http://dx.doi.org/10.1097/00004836-200603000-00015.

[4] Haenen D, Zhang J, Souza da Silva C, Bosch G, van der Meer IM, Van Arkel J, et al. A diet high in resistant starch modulates microbiota composition, SCFA concentrations, and gene expression in pig intestine. J Nutr 2013;143:274–83. http://dx.doi.org/10.3945/jn.112.169672.butyrate.

[5] Levrat M-A, Rémésy C, Demigné C. High propionic acid fermentations and mineral accumulation in the cecum of rats adapted to different levels of inulin. J Nutr 1991;121:1730–7.

[6] Perrin P, Pierre F, Patry Y, Champ M, Berreur M, Pradal G, et al. Only fibres promoting a stable butyrate producing colonic ecosystem decrease the rate of aberrant crypt foci in rats. Gut 2001;48:53–61. http://dx.doi.org/10.1136/gut.48.1.53.

[7] Arora T, Sharma R, Frost G. Propionate. Anti-obesity and satiety enhancing factor? Appetite 2011;56:511–5. http://dx.doi.org/10.1016/j.appet.2011.01.016.

[8] Fung KYC, Cosgrove L, Lockett T, Head R, Topping DL. A review of the potential mechanisms for the lowering of colorectal oncogenesis by butyrate. Br J Nutr 2012;108:820–31. http://dx.doi.org/10.1017/S0007114512001948.

[9] Hamer HM, Jonkers D, Venema K, Vanhoutvin S, Troost FJ, Brummer RJ. Review article: the role of butyrate on colonic function. Aliment Pharmacol Ther 2008;27:104–19. http://dx.doi.org/10.1111/j.1365-2036.2007.03562.x.

[10] Hosseini E, Grootaert C, Verstraete W, Van de Wiele T. Propionate as a health-promoting microbial metabolite in the human gut. Nutr Rev 2011;69:245–58. http://dx.doi.org/10.1111/j.1753-4887.2011.00388.x.

[11] Hove H, Nordgaard-Andersen I, Mortensen PB. Effect of lactic acid bacteria on the intestinal production of lactate and short-chain fatty acids, and the absorption of lactose. Am J Clin Nutr 1994;59:74–9.

[12] Borthakur A, Priyamvada S, Kumar A, Natarajan AA, Gill RK, Alrefai WA, et al. A novel nutrient sensing mechanism underlies substrate-induced regulation of monocarboxylate transporter-1. Am J Physiol Gastrointest Liver Physiol 2012;303:G1126–33. http://dx.doi.org/10.1152/ajpgi.00308.2012.

[13] Hadjiagapiou C, Schmidt L, Dudeja PK, Layden TJ, Ramaswamy K. Mechanism(s) of butyrate transport in Caco-2 cells: role of monocarboxylate transporter 1. Am J Physiol Gastrointest Liver Physiol 2000;279:G775–80.

[14] Kirat D, Kato S. Monocarboxylate transporter 1 (MCT1) mediates transport of short-chain fatty acids in bovine caecum. Exp Physiol 2006;91:835–44. http://dx.doi.org/10.1113/expphysiol.2006.033837.

[15] Stein J, Zores M, Schröder O. Short-chain fatty acid (SCFA) uptake into Caco-2 cells by a pH-dependent and carrier mediated transport mechanism. Eur J Nutr 2000;39:121–5. http://dx.doi.org/10.1007/s003940070028.

[16] Halestrap AP, Price NT. The proton-linked monocarboxylate transporter (MCT) family: structure, function and regulation. Biochem J 1999;343:281–99. http://dx.doi.org/10.1042/0264-6021:3430281.

[17] Gill RK, Saksena S, Alrefai WA, Sarwar Z, Goldstein JL, Carroll RE, et al. Expression and membrane localization of MCT isoforms along the length of the human intestine. Am J Physiol Cell Physiol 2005;289:C846–52. http://dx.doi.org/10.1152/ajpcell.00112.2005.

[18] Ziegler K, Kerimi A, Poquet L, Williamson G. Butyric acid increases transepithelial transport of ferulic acid through upregulation of the monocarboxylate transporters SLC16A1 (MCT1) and SLC16A3 (MCT4). Arch Biochem Biophys 2016;1:1–10. http://dx.doi.org/10.1016/j.abb.2016.01.018.

[19] Buyse M, Sitaraman SV, Liu X, Bado A, Merlin D. Luminal leptin enhances CD147/MCT-1-mediated uptake of butyrate in the human intestinal cell line Caco2-BBE. J Biol Chem 2002;277:28182–90. http://dx.doi.org/10.1074/jbc.M203281200.

[20] Kirat D, Kondo K, Shimada R, Kato S. Dietary pectin up-regulates monocaboxylate transporter 1 in the rat gastrointestinal tract. Exp Physiol 2009;94:422–33. http://dx.doi.org/10.1113/expphysiol.2009.046797.

[21] Hsu CL, Yen GC. Phenolic compounds: evidence for inhibitory effects against obesity and their underlying molecular signaling mechanisms. Mol Nutr Food Res 2008;52:53–61. http://dx.doi.org/10.1002/mnfr.200700393.

[22] Manach C, Mazur A, Scalbert A. Polyphenols and prevention of cardiovascular diseases. Curr Opin Lipidol 2005;16:77–84.

[23] Middleton EJ, Kandaswami C, Theoharides TC. The effects of plant flavonoids on mammalian cells: implications for inflammation, heart disease, and cancer. Pharmacol Rev 2000;52:673–751.

[24] Tomas-Barberan FA, Clifford MA. Flavanones, chalcones and dihydrochalcones — nature, occurrence and dietary burden. J Sci Food Agric 2000;80:1073–80. http://dx.doi.org/10.1002/(SICI)1097-0010(20000515).

[25] Bredsdorff L, Nielsen ILF, Rasmussen SE, Cornett C, Barron D, Bouisset F, et al. Absorption, conjugation and excretion of the flavanones, naringenin and hesperetin from alpha-rhamnosidase-treated orange juice in human subjects. Br J Nutr 2010;103:1602–9. http://dx.doi.org/10.1017/S0007114509993679.

[26] Jin MJ, Kim U, Kim IS, Kim Y, Kim D-H, Han SB, et al. Effects of gut microflora on pharmacokinetics of hesperidin: a study on non-antibiotic and pseudo-germ-free rats. J Toxicol Environ Health A 2010;73:1441–50. http://dx.doi.org/10.1080/15287394.2010.511549.

[27] Brand W, van der Wel PA, Rein MJ, Barron D, Williamson G, van Bladeren PJ, et al. Metabolism and transport of the citrus flavonoid hesperetin in Caco-2 cell monolayers. Drug Metab Dispos 2008;36:1794–802. http://dx.doi.org/10.1124/dmd.107.019943.and.

[28] Brand W, Oosterhuis B, Krajcsi P, Barron D, Dionisi F, van Bladeren PJ, et al. Interaction of hesperetin glucuronide conjugates with human BCRP, MRP2 and MRP3 as detected in membrane vesicles of overexpressing baculovirus-infected Sf9 cells. Biopharm Drug Dispos 2011;32:530–5. http://dx.doi.org/10.1002/bdd.

[29] Sun H, Wang X, Zhou X, Lu D, Ma Z, Wu B. Multidrug resistance-associated protein 4 (MRP4/ABCC4) controls efflux transport of hesperetin sulfates in sulfotransferase. Drug Metab Dispos 2015;43:1430–40.

[30] Brouns F, Hemery Y, Price R, Anson NM. Wheat Aleurone: separation, composition, health aspects, and potential food use. Crit Rev Food Sci Nutr 2012;52:553–68. http://dx.doi.org/10.1080/10408398.2011.589540.

[31] Andreasen MF, Kroon PA, Williamson G, Garcia-Conesa M-T. Esterase activity able to hydrolyze dietary antioxidant hydroxycinnamates is distributed along the intestine of mammals. J Agric Food Chem 2001;49:5679–84.

[32] Kroon PA, Faulds CB, Ryden P, Robertson JA, Williamson G. Release of covalently bound ferulic acid from fiber in the human colon. J Agric Food Chem 1997;45:661–7.

[33] Konishi Y, Shimizu M. Transepithelial transport of ferulic acid by monocarboxylic acid transporter in Caco-2 cell monolayers. Biosci Biotechnol Biochem 2003;67:856–62. http://dx.doi.org/10.1271/bbb.67.856.

[34] Wong CC, Meinl W, Glatt HR, Barron D, Stalmach A, Steiling H, et al. In vitro and in vivo conjugation of dietary hydroxycinnamic acids by UDP-glucuronosyltransferases and sulfotransferases in humans. J Nutr Biochem 2010;21:1060–8. http://dx.doi.org/10.1016/j.jnutbio.2009.09.001.

[35] Tamura H-O, Taniguchi K, Hayashi E, Hiyoshi Y, Nagai F. Expression profiling of sulfotransferases in human cell lines derived from extra-hepatic tissues. Biol Pharm Bull 2001;24:1258–62. http://dx.doi.org/10.1248/bpb.24.1258.

[36] Wong CC, Barron D, Orfila C, Dionisi F, Krajcsi P, Williamson G. Interaction of hydroxycinnamic acids and their conjugates with organic anion transporters and ATP-binding cassette transporters. Mol Nutr Food Res 2011;55:979–88. http://dx.doi.org/10.1002/mnfr.201000652.

[37] Neuhoff S, Ungell AL, Zamora I, Artursson P. pH-dependent passive and active transport of acidic drugs across Caco-2 cell monolayers. Eur J Pharm Sci 2005;25:211–20. http://dx.doi.org/10.1016/j.ejps.2005.02.009.

[38] Ahlin G, Hilgendorf C, Karlsson J, Szigyarto C, Uhlen M, Artursson P. Endogenous gene and protein expression of drug-transporting proteins in cell lines routinely used in drug discovery programs. Drug Metab Dispos 2009;37:2275–83. http://dx.doi.org/10.1124/dmd.109.028654.

[39] Brand W, Boersma MG, Bik H, Hoek-van den Hil EF, Vervoort J, Barron D, et al. Phase II metabolism of hesperetin by individual UDP- glucuronosyltransferases and sulfotransferases and rat and human tissue samples. Drug Metab Dispos 2010;38:617–25. http://dx.doi.org/10.1124/dmd.109.031047.phloridzin.

[40] Lévèques A, Actis-Goretta L, Rein MJ, Williamson G, Dionisi F, Giuffrida F. UPLC-MS/MS quantification of total hesperetin and hesperetin enantiomers in biological matrices. J Pharm Biomed Anal 2012;57:1–6. http://dx.doi.org/10.1016/j.jpba.2011.08.031.

[41] Poquet L, Clifford MN, Williamson G. Transport and metabolism of ferulic acid through the colonic epithelium. Drug Metab Dispos 2008;36:190–7. http://dx.doi.org/10.1124/dmd.107.017558.

[42] Li X, Shang L, Wu Y, Abbas S, Li D, Netter P, et al. Identification of the human UDP-glucuronosyltransferase isoforms involved in the glucuronidation of the phytochemical ferulic acid. Drug Metab Pharmacokinet 2011;26:341–50. http://dx.doi.org/10.2133/dmpk.DMPK-10-RG-125.

[43] Prime-Chapman HM, Fearn RA, Cooper AE, Moore V, Hirst BH. Differential multidrug resistance-associated protein 1 through 6 isoform expression and function in human intestinal epithelial Caco-2 cells. J Pharmacol Exp Ther 2004;311:476–84. http://dx.doi.org/10.1124/jpet.104.068775.important.

[44] Taipalensuu J, Törnblom H, Lindberg G, Einarsson C, Sjöqvist F, Melhus H, et al. Correlation of gene expression of ten drug efflux proteins of the ATP-binding cassette transporter family in normal human jejunum and in human intestinal epithelial Caco-2 cell monolayers. J Pharmacol Exp Ther 2001;299:164–70.

[45] Davie JR. Inhibition of histone deacetylase activity by butyrate. J Nutr 2003;133:2485S–93S.

[46] Steliou K, Boosalis MS, Perrine SP, Sangerman J, Faller DV. Butyrate histone deacetylase inhibitors. Biores Open Access 2012;1:192–8. http://dx.doi.org/10.1089/biores.2012.0223.

[47] Tang Y, Chen Y, Jiang H, Robbins GT, Nie D. G-protein-coupled receptor for short-chain fatty acids suppresses colon cancer. Int J Cancer 2011;128:847–56. http://dx.doi.org/10.1002/ijc.25638.

[48] Wächtershäuser A, Stein J. Butyrate-induced differentiation of Caco-2 cells occurs independently from p27. Biochem Biophys Res Commun 2001;281:295–9. http://dx.doi.org/10.1006/bbrc.2001.4346.

[49] Priyamvada S, Anbazhagan A, Chatterjee I, Alrefail W, Dudeja P, Borthakur A. Gut bacterial metabolite propionate upregulates intestinal epithelial Kruppel-like factor 4 expression *via* a PPAR-γ-dependent mechanism. FASEB J 2015;29.

[50] Runge-Morris M, Kocarek TA. Regulation of sulfotransferase and UDP-glucuronosyltransferase gene expression by the PPARs. PPAR Res 2009;2009. http://dx.doi.org/10.1155/2009/728941.

[51] Runge-Morris M, Kocarek TA, Falany CN. Regulation of the cytosolic sulfotransferases by nuclear receptors. Drug Metab Rev 2013;45:15–33. http://dx.doi.org/10.3109/03602532.2012.748794.

[52] Rondini EA, Pant A, Kocarek TA. Transcriptional regulation of cytosolic sulfotransferase (SULT) 1C2 by intermediates of the cholesterol biosynthetic pathway in primary cultured rat hepatocytes. J Pharmacol Exp Ther 2015;355:429–41. http://dx.doi.org/10.1124/jpet.115.226365.

[53] Jeong H, Choi S, Song J, Chen H, Fischer JH. Regulation of UDP-glucuronosyltransferase (UGT) 1A1 by progesterone and its impact on labetalol elimination. Xenobiotica 2008;38:62–75.
[54] Wen X, Donepudi AC, Thomas PE, Slitt AL, King RS, Aleksunes LM. Regulation of hepatic phase II metabolism in pregnant mice. J Pharmacol Exp Ther 2013;344:244–52. http://dx.doi.org/10.1124/jpet.112.199034.
[55] Bird AR, Hayakawa T, Marsono Y, Gooden JM, Record IR, Correll RL, et al. Coarse brown rice increases fecal and large bowel short-chain fatty acids and starch but lowers calcium in the large bowel of pigs. J Nutr 2000;130:1780–7.
[56] Unno T, Hisada T, Takahashi S. Hesperetin modifies the composition of fecal microbiota and increases cecal levels of short-chain fatty acids in rats. J Agric Food Chem 2015;63:7952–7. http://dx.doi.org/10.1021/acs.jafc.5b02649.